Design of isoplanatic aspheric monofocal intraocular lenses

Sergio Barbero,* Susana Marcos, Javier Montejo and Carlos Dorronsoro

Instituto de Óptica, Consejo Superior de Investigaciones Científicas (CSIC), Serrano 121, 28006 Madrid, Spain.
**sergio.barbero@io.cfmac.csic.es*

Abstract: A new and complete methodology of monofocal intraocular lens (IOL) design is presented aiming at isoplanatism, i.e. IOLs that provide the eye with optimized optical quality over a wide field of view (typically in a range of ten degrees). The methodology uses a merit function considering dimensional and biomechanical constraints, and a geometrical optical quality metric that is evaluated simultaneously at different field angles. As an example, we present new isoplanatic designs based on different commercial IOL platforms. Aspheric isoplanatic designs improve peripheral quality over current aspheric IOLs. Also, isoplanatic designs provide more stable optical quality across the field and across pupil diameter.

OCIS codes: (220.3620) Lens design; (220.4830) Optical system design; (330.4460) Ophthalmic optics and devices; (330.7310) Vision.

References and Links

1. S. Barbero and S. Marcos, "Analytical tools for customized design of monofocal intraocular lenses," Opt. Express **15**(14), 8576–8591 (2007), http://www.opticsinfobase.org/oe/abstract.cfm?URI=oe-15-14-8576.
2. S. Norrby, P. Artal, P. A. Piers, and M. Van der Mooren, Methods of obtaining ophthalmic lenses providing the eye with reduced aberrations " US Patent 6,609,793.
3. M. Gerlach and C. Lesage, "Aspheric intraocular lens and method for designing such IOL" WO Patent 2007/128423.
4. G. E. Altmann and G. Altmann, "Aspheric lens and lens family" WO Patent 2005/203619.
5. R. B. Rabbetts, *Bennett & Rabbetts' clinical visual optics* (Elsevier/Butterworth Heinemann, Edinburgh; New York, 2007).
6. S. Marcos, S. A. Burns, P. M. Prieto, R. Navarro, and B. Baraibar, "Investigating sources of variability of monochromatic and transverse chromatic aberrations across eyes," Vision Res. **41**(28), 3861–3871 (2001).
7. W. N. Charman and D. A. Atchison, "Decentred optical axes and aberrations along principal visual field meridians," Vision Res. **49**(14), 1869–1876 (2009).
8. R. Navarro, E. Moreno, and C. Dorronsoro, "Monochromatic aberrations and point-spread functions of the human eye across the visual field," J. Opt. Soc. Am. A **15**(9), 2522–2529 (1998).
9. G. Smith and C. W. Lu, "Peripheral power errors and astigmatism of eyes corrected with intraocular lenses," Optom. Vis. Sci. **68**(1), 12–21 (1991).
10. J. Tabernero, P. Piers, and P. Artal, "Intraocular lens to correct corneal coma," Opt. Lett. **32**(4), 406–408 (2007).
11. D. A. Atchison, "3rd-Order Aberrations Of Pseudophakic Eyes," Oph. Phy. Opt **9**(2), 205–211 (1989).
12. D. A. Atchison, "Optical design of intraocular lenses. II. Off-axis performance," Optom. Vis. Sci. **66**(9), 579–590 (1989).
13. S. Aoshima, T. Nagata, and A. Minakata, "Optical characteristics of oblique incident rays in pseudophakic eyes," J. Cataract Refract. Surg. **30**(2), 471–477 (2004).
14. R. A. Applegate, J. D. Marsack, R. Ramos, and E. J. Sarver, "Interaction between aberrations to improve or reduce visual performance," J. Cataract Refract. Surg. **29**(8), 1487–1495 (2003).
15. P. de Gracia, C. Dorronsoro, E. Gambra, G. Marin, M. Hernández, and S. Marcos, "Combining coma with astigmatism can improve retinal image over astigmatism alone," Vision Res. **50**(19), 2008–2014 (2010).
16. J. S. McLellan, P. M. Prieto, S. Marcos, and S. A. Burns, "Effects of interactions among wave aberrations on optical image quality," Vision Res. **46**(18), 3009–3016 (2006).
17. I. Gontijo, A. Ossipov, and T. R. Paul, "Optimizing intraocular lens" WO Patent 2009/142961.
18. D. T. Azar, *Intraocular lenses in cataract and refractive surgery* (Saunders, Philadelphia, 2001).
19. S. Marcos, P. Rosales, L. Llorente, and I. Jiménez-Alfaro, "Change in corneal aberrations after cataract surgery with 2 types of aspherical intraocular lenses," J. Cataract Refract. Surg. **33**(2), 217–226 (2007).
20. C. W. Lu and G. Smith, "The Aspherizing Of Intraocular Lenses," Oph. Phy. Opt. **10**(1), 54–66 (1990).
21. C. Pagnoulle, S. Nolet De Brauwere Van, C. R. M. Pagnoulle, and S. T. Nolet De Brauwere Van, "Polymer composition for an intraocular lens" WO Patent 2006/063994.

#139474 - $15.00 USD Received 9 Dec 2010; revised 9 Feb 2011; accepted 6 Mar 2011; published 18 Mar 2011

22. S. R. Nanushyan, I. Valunin, and E. J. Alexeeva, "High refractive index silicone for use in intraocular lens" US Patent 6432137.
23. C. Freeman, D. L. Jinkerson, M. Karakelle, A. R. Leboeuf, and A. Leboeuf, "High refractive index ophthalmic device materials" WO Patent WO9953347.
24. S. Q. Zhou, J. C. Sy, M. A. Berteig, and T. P. Richards, "High refractive index silicone compositions" US Patent 5444106.
25. S. Barbero, S. Marcos, C. Dorronsoro, J. Montejo, and P. Salazar, "Procedimiento para elaborar una lente intraocular monofocal asferica isoplanática y lente obtenida empleando dicho procedimiento," Spanish patent application P201030855.
26. S. Barbero, "Refractive power of a multilayer rotationally symmetric model of the human cornea and tear film," J. Opt. Soc. Am. A **23**(7), 1578–1585 (2006).
27. K. Kriechbaum, O. Findl, P. R. Preussner, C. Köppl, J. Wahl, and W. Drexler, "Determining postoperative anterior chamber depth," J. Cataract Refract. Surg. **29**(11), 2122–2126 (2003).
28. D. A. Atchison, N. Pritchard, K. L. Schmid, D. H. Scott, C. E. Jones, and J. M. Pope, "Shape of the retinal surface in emmetropia and myopia," Invest. Ophthalmol. Vis. Sci. **46**(8), 2698–2707 (2005).
29. T. Grosvenor and R. Scott, "Role of the axial length/corneal radius ratio in determining the refractive state of the eye," Optom. Vis. Sci. **71**(9), 573–579 (1994).
30. L. Llorente, S. Barbero, D. Cano, C. Dorronsoro, and S. Marcos, "Myopic versus hyperopic eyes: axial length, corneal shape and optical aberrations," J. Vis. **4**(4), 288–298 (2004).
31. D. A. Atchison, "Optical models for human myopic eyes," Vision Res. **46**(14), 2236–2250 (2006).
32. T. Olsen, "Prediction of the effective postoperative (intraocular lens) anterior chamber depth," J. Cataract Refract. Surg. **32**(3), 419–424 (2006).
33. G. W. Forbes, "Optical system assessment for design: numerical ray tracing in the Gaussian pupil," J. Opt. Soc. Am. A **5**(11), 1943–1956 (1988).
34. D. A. Atchison, "Optical design of intraocular lenses. I. On-axis performance," Optom. Vis. Sci. **66**(8), 492–506 (1989).
35. S. S. Lane, P. Burgi, G. S. Milios, M. W. Orchowski, M. Vaughan, and E. Schwarte, "Comparison of the biomechanical behavior of foldable intraocular lenses," J. Cataract Refract. Surg. **30**(11), 2397–2402 (2004).
36. X. Hong, J. Xie, and et. al., "Intraocular lens," (2006).
37. G. E. Altmann, L. D. Nichamin, S. S. Lane, and J. S. Pepose, "Optical performance of 3 intraocular lens designs in the presence of decentration," J. Cataract Refract. Surg. **31**(3), 574–585 (2005).
38. P. Rosales and S. Marcos, "Customized computer models of eyes with intraocular lenses," Opt. Express **15**(5), 2204–2218 (2007), http://www.opticsinfobase.org/oe/abstract.cfm?URI=oe-15-5-2204.
39. J. D. Marsack, L. N. Thibos, and R. A. Applegate, "Metrics of optical quality derived from wave aberrations predict visual performance," J. Vis. **4**(4), 322–328 (2004).
40. S. Marcos, S. Barbero, and I. Jiménez-Alfaro, "Optical quality and depth-of-field of eyes implanted with spherical and aspheric intraocular lenses," J. Refract. Surg. **21**(3), 223–235 (2005).
41. S. Marcos, P. Rosales, L. Llorente, S. Barbero, and I. Jiménez-Alfaro, "Balance of corneal horizontal coma by internal optics in eyes with intraocular artificial lenses: evidence of a passive mechanism," Vision Res. **48**(1), 70–79 (2008).
42. H. L. Liou and N. A. Brennan, "Anatomically accurate, finite model eye for optical modeling," J. Opt. Soc. Am. A **14**(8), 1684–1695 (1997).
43. T. Olsen, "Sources of error in intraocular lens power calculation," J. Cataract Refract. Surg. **18**(2), 125–129 (1992).
44. O. Pomerantzeff, M. M. Pankratov, and G. J. Wang, "Calculation of an IOL from the wide-angle optical model of the eye," J. Am. Intraocul. Implant Soc. **11**(1), 37–43 (1985).
45. P. A. Bedggood, R. Ashman, G. Smith, and A. B. Metha, "Multiconjugate adaptive optics applied to an anatomically accurate human eye model," Opt. Express **14**(18), 8019–8030 (2006), http://www.opticsinfobase.org/abstract.cfm?URI=oe-14-18-8019.
46. M. A. Nanavaty, D. J. Spalton, J. Boyce, S. Saha, and J. Marshall, "Wavefront aberrations, depth of focus, and contrast sensitivity with aspheric and spherical intraocular lenses: fellow-eye study," J. Cataract Refract. Surg. **35**(4), 663–671 (2009).
47. J. Kumler, "Designing and specifying aspheres for manufacturability," in *Current Developments in Lens Design and Optical Engineering VI*(SPIE, San Diego, CA, USA, 2005), pp. 58740C–58749.
48. A. Y. Anis, "Flexible posterior chanber lens," US Patent 4880427.
49. M. Dubbelman and G. L. Van der Heijde, "The shape of the aging human lens: curvature, equivalent refractive index and the lens paradox," Vision Res. **41**(14), 1867–1877 (2001).
50. A. Patz, "Photocoagulation of retinal, vascular, and macular diseases through intraocular lenses," Ophthalmology **88**(5), 398–406 (1981).
51. R. M. Kershner, "Retinal image contrast and functional visual performance with aspheric, silicone, and acrylic intraocular lenses. Prospective evaluation," J. Cataract Refract. Surg. **29**(9), 1684–1694 (2003).

1. Introduction

Intraocular lenses (IOLs) are normally implanted in cataract surgery to replace the opaque crystalline lens, and to correct for the refractive error of the eye. Typically, monofocal IOLs are implanted to achieve emmetropia for far vision. However the optical quality of a

#139474 - $15.00 USD Received 9 Dec 2010; revised 9 Feb 2011; accepted 6 Mar 2011; published 18 Mar 2011

pseudoaphakic eye (after IOL implantation) is determined, not only by the refractive error (defocus), but also by optical aberrations. As a consequence, controlling the optical aberrations is a main target in IOL design.

Earlier IOL designs only made use of spherical surfaces. However, as spherical intraocular lenses induce spherical aberration, which adds to the normally positive spherical aberration of the eye, most current designs incorporate aspheric surfaces. Introducing aspheric surfaces provides new degrees of freedom to achieve a better optical performance. In addition, aspherizing the IOL surfaces also allow a reduction of the lens volume, with advantages in the implantation of the IOL through smaller incisions. We had previously [1] pointed out that aspherizing the posterior surface can be a strategy to reduce the IOL central thickness.

A great number of IOL manufacturing companies commercialize aspheric IOLs, generally with the aim of reducing the amount of ocular spherical aberration on axis. For example, the Tecnis^{TM} CL Z9002 [2] (Pharmacia) and the CT ASPHINA 603P [3] (Carl Zeiss) lenses are designed to cancel the spherical aberration of a pseudoapakic eye model. A different criterion is followed in the SoftPort IOL [4] (Bausch and Lomb), where rather than cancelling the spherical aberration of the average cornea, it aims at cancelling the spherical aberration for a bundle of rays coming parallel with respect to the optical axis.

However, introducing aspheric surfaces provides the potential for controlling optical aberrations not only on-axis, but also off-axis. The human eye does not have a well-defined optical axis because its surfaces are not rotationally symmetric and as a result of the foveal eccentric position. Normally, the line of sight ─ the axis joining the fovea with the pupil center ─ defines the so-called optical quality on-axis. Therefore, in practice, the axis of rotational symmetry of an IOL can be different from the line of sight. The angle between both axes is on average around 5° [5], although there are significant differences across subjects [6]. In consequence, the optical quality off-axis must be considered [7].

The optical quality of the young phakic eye [8] is relatively constant across the central visual field (within around 10 deg), hence the human eye can be considered an isoplanatic optical system. Therefore, isoplanatic IOLs should outperform designs considering only on-axis aberrations and, in terms of off-axis optical quality, mimic the performance of young phakic eyes.

Although some previous works have studied off-axis aberrations for different IOL designs [9–11], few studies in the literature propose design methods aiming at providing optimal overall image quality both on and off-axis. From third order aberration theory, it is known that for small field angles the two major aberrations are coma and spherical aberration [11,12]. Hence, Tabernero et al [10] have proposed IOL designs with simultaneous correction of spherical aberration and lateral coma. However, peripheral power errors (field curvature) and astigmatism can also contribute importantly to the off-axis performance even for small angles [9,13], especially when considering retinal shape. Smith et al [9] proposed a design optimized to correct peripheral power errors and oblique astigmatism. These previous studies have in common that they focused on the correction of specific refractive errors or aberrations, but not on the overall optical quality. An alternative strategy to the correction of individual aberrations is the optimization of the overall image quality, which we propose in the current study.

This approach considers all the aberrations together, as well as potential interactions across terms [14–16]. Despite its advantages, this approach has not been sufficiently considered in IOL design. To our knowledge, only a proposal in the patent literature mentions the possibility of correcting global aberrations on-axis and off-axis [17]. We propose new IOL designs where optical aberrations are minimized in a wide field of view (up to 10 °).

Most of the existing aspheric designs have either surfaces described by simple conics – two design parameters: the vertex radius of curvature and the conic constant – or surfaces described by general aspheric surfaces using two or three extra aspheric coefficients, besides the parameters of the conic. To our knowledge, the implications of using one or the other surface type have not been reported. The current study will provide a systematic analysis of

#139474 - $15.00 USD Received 9 Dec 2010; revised 9 Feb 2011; accepted 6 Mar 2011; published 18 Mar 2011

the advantages of using general aspheric surfaces as opposed to simple conical and spherical surfaces.

Besides the control of optical aberrations, IOL design is limited by a set of boundary conditions that constraint the optimal optical designs. First, the physical dimensions and the biomechanical properties of the lens must be considered. Small and highly foldable IOLs allow to reduce the incision size in cataract surgery, which reduces the risk of postoperative inflammation [18] and the generation of corneal optical aberrations [19]. The volume of the IOL limits the minimum attainable insertion incision. Reducing the volume of the IOL mainly implies to reduce the central thickness ─ the edge thickness is usually set to a specific value in order to secure the haptic mechanical stability. As a result of reducing thickness, and in order to achieve the necessary optical power, higher refractive indices are needed. However, the increase of refractive index may result in an increase of glare effects due to surface reflections [20]. In addition, extremely thin or foldable IOLs are less mechanically stable and may shift their optimal axial location inside the eye. In summary, as a result of trade-offs in the design parameters of IOLs, it is necessary to include boundary conditions which restrict the admissible central and edge IOL thickness in the design procedure.

Another critical aspect of IOLs relates to the lens material [21–24]. Today, the most popular materials are acrylic and silicones, which can be hydrophobic or hydrophilic. Refractive indices range from 1.55 (Acrysof® lenses by Alcon [23]) to 1.46 (CeeOn® patented by Pharmacia [24] and IolTech® by Carl Zeiss) and 1.43 (SoFleX® LI61U by Bausch & Lomb). Finally, the IOLs are placed in the eye by means of the haptics, which can come in multiple designs [18]. The thickness of the haptic sets the edge thickness for the IOL. For the purpose of this study, we refer to "IOL platform" as that defined by the dimensions of the IOL (IOL optical diameter and edge thickness) and the refractive index of the material.

In this study we present a new IOL design methodology [25] based on the optimization of a global optical quality metric in an extended field of view. The new methodology considers a set of boundary conditions. As an example of the potential of the methodology, we present several new IOL designs (optical power of 22 D) for different existing IOL platforms, and compare the theoretical optical performance of the these designs with respect to its commercial counterparts.

2. Methods

The optical design methodology comprises the following steps: 1) Building of a pseudoaphakic computer eye model. 2) Definition of a merit function, by means of an optical target and several boundary conditions. 3) Optimization of the IOL design parameters.

2.1 Pseudophakic eye model

We employed a generic pseudoaphakic eye model [1] based on biometric data extracted from the literature. The model is composed of a set of concentric surfaces described by conics defined by: $y^2 = 2Rz-(1 + Q)z^2$, where R denotes the apical radius, Q the asphericity, and y and z represent lateral and axial coordinates respectively. The parameters used are described in Table 1.

We modeled the cornea as a multilayer structure comprising three layers with different indices of refraction: tear film, epithelium and an extended stroma, as described by Barbero [26]. We set the location of the entrance pupil of the eye model 0.9 mm behind the anterior surface of the IOL, as proposed in a previous study [2]. For the anterior chamber depth (defined as the distance from the posterior surface of the cornea to the anterior surface of the IOL) we took an average value of 4.11 mm from Kriechbaum et al. study [27].

A specific feature of the model is the use of a curved retina to consider the wide field optical performance. In particular, the retina is described by a conic surface, based on the data provided by Atchison et al [28]. In Atchison's study [28], the retina was measured in 21 emmetropic eyes using Magnetic Resonance Imaging, and its shape subsequently fitted by ellipsoids described by the radius of curvature and asphericity in the vertical and horizontal meridians.

#139474 - $15.00 USD Received 9 Dec 2010; revised 9 Feb 2011; accepted 6 Mar 2011; published 18 Mar 2011

2.2. Pseudoaphakic eye model for an IOL of a given optical power

Monofocal IOLs come in a range of optical powers. Selection of the optimal optical power requires measurement of biometric parameters of the patient eye and assumption of a fixed post-operative IOL position. The selection of the IOL optical power is aimed at correcting on-axis refraction. In consequence, the pseudoaphakic eye model used to design the IOLs must be free of defocus error on-axis. For a fixed optical power in the IOL, cancelation of defocus can be achieved by tuning the axial length, the lens position or the corneal power, as all those parameters affect the total eye power. To our knowledge a procedure to define defocus-corrected pseudoaphakic eye models with different IOL powers has not been fully described in the literature.

We propose a method for designing IOLs of different powers in a set of model eyes. For each IOL power, two parameters of the model (axial length and the retina shape) are adaptively modified, taking into account reported relationships between refractive error and axial length [29,30], and the close relation between retinal shape with the axial length [31].

The procedure comprises two different steps. First, an initial axial length value of 23.08 mm is assumed (which corresponds to the average axial length across 6698 patients reported by Olsen et al. [32]). The IOL is initially assumed to be a biconvex lens with a thickness equal to the maximum allowed value. Second, the axial length is changed in an optimization procedure that cancels the defocus term in the pseudoaphakic eye model of Table 1 with the initial biconvex IOL geometry. Finally, the retina shape is modified according to the equations of Atchison et al [31] that relates axial length with refraction and with retina shape.

Calculations were performed for a pupil diameter of 4-mm, as justified elsewhere [26].

Table 1. Parameters of a generic pseudoaphakic eye model.

Interface						
	Air-Tear	Tear-Epithelium	Epithelium-Stroma	Stroma-Aqueous	Retina	
R	7.79	7.79	7.556	6.53	V	
Q	–0.015	–0.015	–1.43	–0.455	V	
Medium						
	Tear	Epithelium	Stroma	Aqueous	IOL	Vitreous
CT	0.004	0.054	0.473	4.11	O	V
n	1.337	1.376	1.376	1.337	nIOL	1.337

R and Q denotes the apical radius (mm) an the asphericity respectively. CT denotes central thickness in mm. The refractive indices (n) are for a 555-nm wavelength at 37°C. V means that it depends on axial length. O denotes an optimization parameter. nIOL is the refractive index of the IOL material

2.3. Merit function construction: Optical target

The merit function defines mathematically the optical target of the design procedure, considering the boundary conditions.

The optical target was defined as an optical quality metric evaluated simultaneously across a given field of view. We analyzed the optical performance using geometrical ray tracing, computed with the program Zemax V.9 (Focus Software, Tucson, AZ). We used a quality metric derived from the ray tracing procedure. Specifically, we used the root-mean square wavefront error (RMS) of the wavefront for a single wavelength, which allows fast computations. The RMS can be evaluated with respect to the chief ray or the centroid (the point which minimizes the variance of the wavefront). We used the centroid in order to cancel the tilt and piston of the wavefront. It should be pointed out that wavefront tilts generate different magnifications for different fields of view (distorsion).

To compute the RMS for a specific field angle it is necessary to define the sampling pattern of the rays going through the entrance pupil. We used a sampling pattern based on a Gauss quadrature, as proposed by Forbes et al [33], and implemented in Zemax. The required number of rays depends on the amount and distribution of the aberrations of the system.

#139474 - $15.00 USD Received 9 Dec 2010; revised 9 Feb 2011; accepted 6 Mar 2011; published 18 Mar 2011

Following the recommendation procedure by Zemax (Zemax User's Guide February 3 2005) we found that 24 rays per field angle (Gauss quadrature with 3 rings and 6 arms) provided an accurate computation. This is close to the number proposed by Atchison [34] who used 10 rays on-axis and 25 off-axis to evaluate the optical performance of a pseudoaphakic eye.

The optical target was defined with the equation: $\sum_{i=1}^{5} w_i RMS_i$, where RMS_i represents the RMS for field angle i, and w_i are the weights (relative importance) given to each RMS. We found that an optimal optical target is defined when the field angles are 0°, 2.5°, 5°, 7.5° and 10°, with weights 5, 1, 1, 1 and 10 respectively. This optical target is a trade-off between resultant isoplanatism, overall optical quality and computation time.

2.4. Merit function construction: Boundary conditions

The design parameters of the IOL are the variable parameters of the merit function. The range of variation of these values is limited by the boundary conditions.

The first boundary condition enforces that the IOL geometry must provide a specific IOL power. This limits the combination of radii and central thickness of the IOL. The introduction of this boundary condition in the merit function was achieved by algebraic combinations of several operands relating the radii of curvature with the central thickness.

Constraints to the thickness were used to limit the dimensions of the lens. A maximum and minimum threshold for the central and edge thickness of the IOL were selected, specific for each IOL platform. We also enforced a constraint to the IOL vault (total maximum thickness). On the one hand, large vault values provide a higher degree of freedom in the surfaces design, but on the other hand the resulting lens could have excessively curved surfaces, which could result in longitudinal IOL displacement from mechanical haptic forces [35].

Finally we also set a maximum value to the conic constant of the anterior and posterior IOL surface to avoid surface profiles with inflection points, which could generate optical undesired reflections.

2.5. Optimization procedure

Once the merit function is defined, finding its minimum provides the desired combination of designed parameters. The minimum of the merit function was found by applying an optimization routine. However, the merit function defined in the previous section is very complex because it contains a large number of designed parameters (up to eleven in aspheric IOLs) and six boundary constraints. Trying to find the minimum in a single optimization step did not provide the best results. To solve this problem, we designed an optimization procedure divided in two sequential steps. First, we optimized the merit function with only the radii of curvature and the central thickness as variable parameters, using the associated equi-convex lens for the given power as the starting point for the optimization. Second, using as initial values those obtained in the first step, we optimized all the design parameters.

For the optimization algorithm, we employed a combination of classical damped least squares and Hammer algorithms implemented in Zemax (Zemax User's Guide February 3 2005). The Hammer algorithm uses an iterative procedure of adjustments and optimizations in order to perform an exhaustive search for the minimum of the merit function. We used it as the final step of the optimization procedure.

3. Example of application of the design methodology

3.1 IOL-baseline platforms

To show the potential of the new design methodology we designed 22-D IOLs corresponding to different commercial platforms. We selected a 22-D IOL because, for this power, the complete geometry information is typically available from patent descriptions of commercial IOLs. We generated new isoplanatic designs based on the baseline platforms of several commercial lenses, and compared the optical performance of the original designs with that of the new designs, on the same computer eye models.

#139474 - $15.00 USD Received 9 Dec 2010; revised 9 Feb 2011; accepted 6 Mar 2011; published 18 Mar 2011

Specifically, we analyzed four spherical designs: SA60AT from Alcon [36], CeeOn Edge 911 [2,24] from Pharmacia, LI61U from Bausch & Lomb [4,37]; and four aspheric designs: Tecnis Z9002 from Pharmacia [2], AcrySof IQ (Model SN60WF) from Alcon [36], SofPort from Bausch & Lomb (from now on B&L) [4], and CT ASPHINA 603P from Carl Zeiss [3]. Table 2 summarizes the properties of these lenses. Figure 1 shows the surface profiles of the lenses of Table 2.

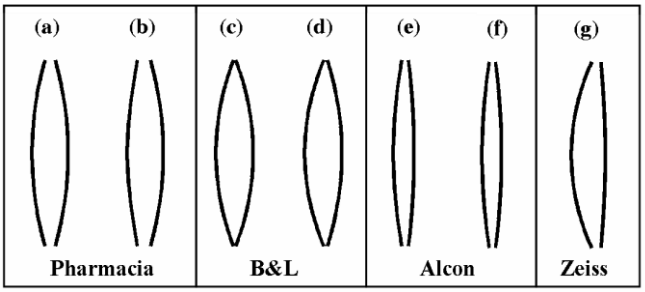

Fig. 1. Surface profiles of 22 D commercial lenses (Table 2): (a) CeeOn (Pharmacia) (b) Tecnis (Pharmacia) (c) LI61U (B&L) (d) SofPort (B&L) (e) SA60AT (Alcon) (f) SN60WF (Alcon) (g) XL-Stabi-ZO (Zeiss). Anterior surfaces are shown in the left.

The edge thickness, defined as the thickness at the edge of the optical zone, was obtained considering the geometry of the surfaces and the central thickness. The optical zone diameter of the IOL was 6 mm, in all cases.

Using these baseline platforms we obtained new designs using only spherical, conic or aspheric surfaces (described with three aspheric coefficients) using the design methodology described above.

3.2 Computer simulation of the optical performance of the IOL designs

We analyzed the optical performance, through computer simulations on and off-axis, of the commercial and the new IOL designs on pseudophakic eye models. Whereas for the optical design procedure we used a generic pseudoaphakic eye model (explained in section 2.1), the optical evaluation of the designed was performed on individual eye models. These eye models were built using keratometric, anterior chamber and axial length data of a set of 6 eyes from a previous study in our laboratory [19], where 22-D lenses had been implanted. These individual models are rotationally symmetry, and all the surfaces are described by conics.

In addition, in order to assess the contribution of biometric parameters that disrupt the rotational symmetry of the eye models (corneal irregularities, tilt and decentrations of the IOL) into the final optical quality of the new lenses (with respect to previous designs), we used two customized pseudoaphakic eye models. These models considered all the anatomical parameters measured on the patient eyes, including corneal topography, IOL tilt and decentration, and the eccentricity of the fovea. These eye models (eye #1 and eye #2 in Rosales et al [38]) have proved to predict the measured high order aberrations with high accuracy, once all the individual parameters were introduced [38]. In these particular examples, 19.5 D SN60WF (Alcon) aspheric IOLs had been implanted; thus we applied the IOL design methodology to the Alcon platform.

Table 2. IOL parameters of commercial lenses.

IOL model	CT (mm)	ET (mm)	n
CeeOn	1.164	0.333	1.458
TECNIS	1.164	0.428	1.458
LI61U	1.202	0.070	1.427
SofPort	1.206	0.116	1.427

#139474 - $15.00 USD Received 9 Dec 2010; revised 9 Feb 2011; accepted 6 Mar 2011; published 18 Mar 2011

SA60AT	0.668	0.210	1.554		
SN60WF	0.633	0.210	1.554		
XL Stabi ZO	1.1	0.292	1.46		
IOL model	Ra(mm)	Qa	2th a.c.	4th a.c.	6th a.c.
CeeOn	11.043	0	0	0	0
TECNIS	11.043	–1.036	0	–9.4E-4	–1.4E-5
LI61U	8.234	0	0	0	0
SofPort	7.285	–1.086	0	0	0
SA60AT	16.379	0	0	0	0
SN60WF	19.583	0	0	0	0
XL Stabi ZO	7.1497	0	0	0	0
IOL model	Rp (mm)	Qp	2th p.c.	4th p.c.	6th p.c.
CeeOn	–11.043	0	0	0	0
TECNIS	–11.043	0			
LI61U	–8.234	0	0	0	0
SofPort	–9.47	–1.086	0	0	0
SA60AT	–25	0	0	0	0
SN60WF	–20	–33.227	–2.5E-4	–1.7E-5	8.7E-7
XL Stabi ZO	–36.390	0	–6.8E-3	1.0E-3	–6.2E-5

CT and ET denote central and edge thicknesses respectively. Ra and Rp denote the anterior and posterior radii of curvature of the IOL; Qa and Qp denote the anterior and posterior asphericities; 2th, 4th and 6th a.c. and p.c. denote second, fourth and six order aspheric coefficient for the anterior and the posterior surface respectively; n is the refractive index (555 nm) when the IOL is inside the eye (37°C) as given by the manufacturer.

Optical performance in pseudophakic eye models was calculated in terms of RMS as a function of the field of view (up to 10° angle) and for different pupil radius (3, 4 and 5 mm). For comparison purposes, we also evaluated the optical performance in terms of the Strehl ratio, as retinal image quality based metrics have been shown to better correlate with visual performance than RMS [39]. On-axis defocus was cancelled to reveal more clearly the optical quality off-axis.

The uniformity of the IOL performance across the field of view was evaluated computing the difference of RMSs at 10° and 0° of object field angle (for an intermediate pupil size of 4 mm). We named this metric: *FOVU (Field of View Uniformity).* Following the same strategy, we evaluated the uniformity of the IOL optical performance with respect to pupil size changes, computing the difference of RMSs at 5 mm and 3 mm pupil sizes (for an intermediate object field angle of 6°). We named this metric *PSS (Pupil Size Stability).* Low values for these metrics are indicative of high stability across the field and pupil diameter, respectively.

4. Results

4.1 The geometry of the new designs

Table 3 summarizes the design parameters for the spherical, conic and aspheric new 22 D isoplanatic IOLs, obtained for the different commercial base-line platforms.

Table 3. IOL parameters of the new isoplanatic lenses for the different platforms.

IOL model	CT (mm)	ET (mm)	Ra (mm)	Qa	Rp (mm)	Qp

#139474 - $15.00 USD Received 9 Dec 2010; revised 9 Feb 2011; accepted 6 Mar 2011; published 18 Mar 2011

Spherical (Pharmacia)	1.165	0.333	12.442	0	–9.926	0
Conic (Pharmacia)	1.146	0.428	16.341	–20.000	–8.345	–5.599
Aspheric (Pharmacia)	1.173	0.428	10.318	–20.000	–11.874	–16.583
Spherical (B&L)	1.203	0.070	8.926	0	–7.642	0
Conic (B&L)	1.075	0.116	12.399	–13.169	–6.173	–3.506
Aspheric (B&L)	1.098	0.116	9.795	–0.366	–7.109	–20.000
Spherical (Alcon)	0.669	0.21	27.051	0	–15.583	0
Conic (Alcon)	0.614	0.21	32.268	–20	–14.262	–18.837
Aspheric (Alcon)	0.635	0.21	27.289	–20	–15.508	3.844
Spherical (Zeiss)	1.110	0.292	12.726	0	–10.042	0
Conic (Zeiss)	0.999	0.292	16.482	–20	–8.521	–5.776
Aspheric (Zeiss)	1	0.292	10.710	2.193	–11.804	–20
IOL model	2th a.c.	4th a.c.	6th a.c.	2th p.c.	4th p.c.	6th p.c.
Aspheric (Pharmacia)	–2.39E-02	1.21E-03	–4.52E-04	–3.24E-02	–1.40E-03	–2.03E-04
Aspheric (B&L)	1.49E-02	2.89E-03	6.48E-05	3.93E-03	–1.66E-03	5.65E-04
Aspheric (Alcon)	–2.32E-02	–2.73E-03	–1.53E-04	–2.71E-02	–2.32E-03	–1.00E-04
Aspheric (Zeiss)	6.18E-03	1.97E-03	–3.14E-05	1.39E-03	7.21E-04	2.33E-04

CT and ET denote central and edge thicknesses respectively. Ra and Rp denote the anterior and posterior radii of curvature of the IOL. Qa and Qp denote the anterior and posterior asphericities. 2th, 4th and 6th a.c. and p.c. denote second, fourth and six order aspheric coefficient for the anterior and the posterior surface respectively. n is the refractive index (555 nm) when the IOL is inside the eye (37°C) as given by the manufacturer.

Figure 2 shows graphically the surface profiles of the IOLs of Table 3. The new designs clearly differ from the commercial ones (in Fig. 1), especially the aspheric surface profiles, which show steeper curvature changes. Whereas all the commercial IOL designs are biconvex, the new aspheric isoplanatic IOL based on the Alcon platform is a meniscus type.

#139474 - $15.00 USD Received 9 Dec 2010; revised 9 Feb 2011; accepted 6 Mar 2011; published 18 Mar 2011

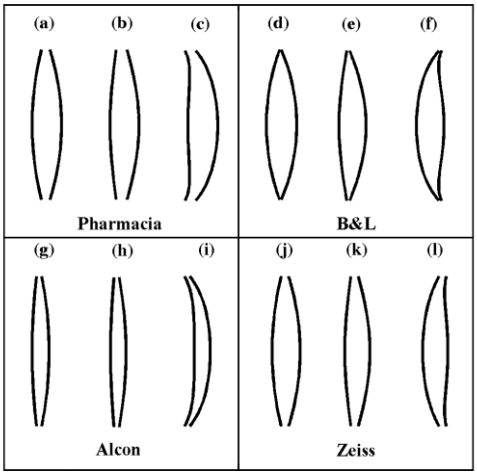

Fig. 2. Surfaces profiles of new 22 D isoplanatic lenses (Table 3) for the Pharmacia platform: (a) spherical (b) conic (c) aspheric, B&L platform (d) spherical (e) conic (f) aspheric, Alcon platform: (g) spherical (h) conic (i) aspheric and Carl Zeiss platform (j) spherical (k) conic (l) aspheric.

4.2 Optical performance of commercial and new IOL designs

The different designs were evaluated on six eyes. We found some intersubject variability in the optical performance of each design. Figure 3 shows the individual performance (RMS as a function of objective field angle) of a commercial IOL (Tecnis-Pharmacia) in the six eyes (for 4-mm pupil). In what follows, average data across the six eyes are provided.

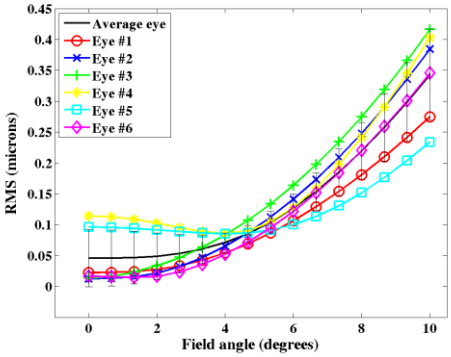

Fig. 3. RMS (microns), as a function of the object field angle (°), for the 6 different eye models where the 22 D Tecnis IOL was implanted. The average and standard deviation are plotted (black lines).

Figure 4 shows the optical performance of the commercial designs of Table 2 (for 4-mm pupils) in terms of RMS as a function of object field angle. For the commercial designs, optical quality was systematically improved from the spherical to aspheric designs, as it has been also shown experimentally [40]. A paired t-test showed the statistical differences between the RMS curves across all subjects. The RMS on-axis (4 mm pupil size) decreased significantly from 0.17 μm (L161U) to 0.11 μm (SofPort) for B&L lenses (*p*-value = 5.47e-5), from 0.15 μm (CeeOn) to 0.05 μm (Tecnis) for Pharmacia lenses (*p*-value = 0.0029), and from 0.13 μm (SA60AT) to 0.04 μm (SN60WF) for Alcon lenses (*p*-value = 2.9e-4).

#139474 - $15.00 USD Received 9 Dec 2010; revised 9 Feb 2011; accepted 6 Mar 2011; published 18 Mar 2011

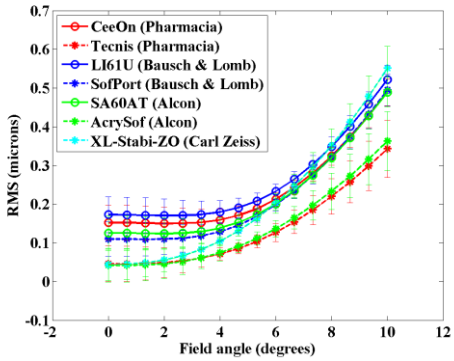

Fig. 4. RMS as a function of objective Acrysof-IQ field angle for the commercial IOL designs (averaged across 6 eyes). Error bars stand for standard deviations.

Aspheric IOL designs showed a benefit for off-axis viewing, as we had also reported experimentally [41]. The RMS off-axis (6° field of angle and 4 mm pupil diameter) decreased from 0.24 μm (L161U) to 0.20 μm (SofPort) for B&L lenses (*p*-value = 2.7e-4), from 0.21 μm (CeeOn) to 0.13 μm (Tecnis) for Pharmacia lenses (*p*-value = 2e-4), and from 0.2 μm (SA60AT) to 0.14 μm (Acrysof-IQ) for Alcon lenses (*p*-value = 7.3 e-4).

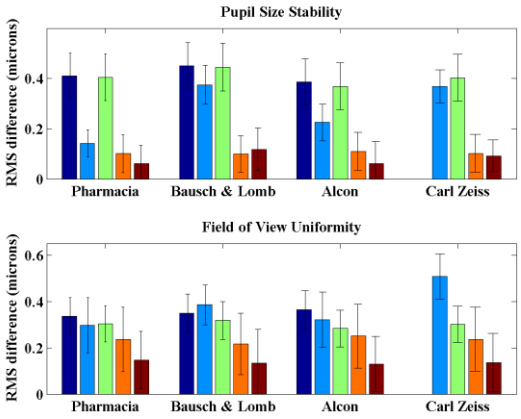

Fig. 5. FOVU and PSS of commercial designs: spherical (dark blue bars) and aspheric (light blue bars) and new isoplanatic designs: spherical (green bars), conic (orange bars) and aspheric (brown bars). Error bars stand for standard deviations.

Figure 5 shows the Field-of-View uniformity (FOVU) the Pupil Size Stability (*PSS*) metrics for all IOL commercial designs. In all the platforms, the aspheric designs have better pupil size and field-of-view stability than their spherical counterparts, except for the B&L lenses where the commercial spherical lens has better FOVU than the aspheric one.

Figure 6 shows the optical performance (4-mm pupil diameter) as a function of the object field angle for the new isoplanatic IOL designs (spherical, conic and aspheric) for the a) Pharmacia b) Alcon c) B&L and d) Zeiss IOL platforms.

#139474 - $15.00 USD Received 9 Dec 2010; revised 9 Feb 2011; accepted 6 Mar 2011; published 18 Mar 2011

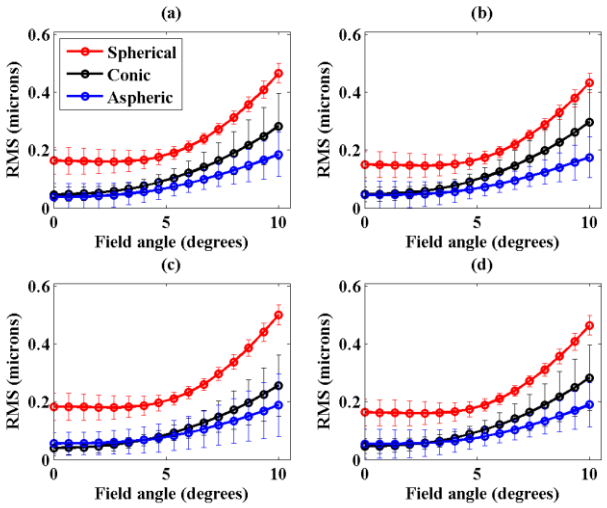

Fig. 6. RMS as a function of the object field angle for the new isoplanatic IOL designs of the Pharmacia b) Alcon c) B&L and d) Zeiss IOL platforms. The spherical, conic and aspheric designs are plotted with red, black and blue lines respectively. Results are averaged across six model eyes. Error bars stand for standard deviations.

As expected, for the four platforms the optical performance of the conic designs is better than the spherical design, and the conic design is further improved by the aspheric design. On average, across the four platforms, the optical quality improvement (average RMS over the central 10 deg of visual field with a 4-mm pupil diameter) with respect to the spherical IOL designs is 49.15% for the conic designs, and 60.94% for the aspheric designs. Moreover, there is also an important improvement in the uniformity of optical performance across the visual field (*FOV*) and pupil size (*PSS*), with the exception of the new conic and aspheric designs based on the B&L baseline platform. For this platform, as shown in Fig. 5 the *PSS* for the aspheric design is slightly worse than for the conic design although this does not occur for the *FOV*.

In order to analyze if the new IOL designs are superior to the state-of the art commercial designs, the optimal isoplanatic IOL designs (those with aspheric surfaces) were compared to the commercial IOLs of Table 2. Figure 7 shows the RMS versus the field of view angle (4 mm pupil diameter) for the four different platforms: a) Pharmacia b) Alcon c) B&L and d) Zeiss IOL platforms. In all cases, the off-axis optical performance of the new isoplanatic designs largely exceeds that of the state-of-the art commercial designs. For 6° field of angle and 4 mm pupil size, RMS off-axis decreased by 32.87% (p-value = 0.0755), 50.21% (p-value = 0.0198), 38.79% (p-value = 0.0077), and a 53.86% (p-value = 0.0016), for the Pharmacia, B&L, Alcon and Carl Zeiss platforms respectively, when comparing the new isoplanatic design and the aspheric commercial design. In addition the FOVU improves in the new designs by 54.65%, 66.25%, 72.86%, 74.74%, and the *PSS* by 53.27%, 66.73%, 59.65%, 71.84% for the Pharmacia, B&L, Alcon and Carl Zeiss platforms respectively.

#139474 - $15.00 USD Received 9 Dec 2010; revised 9 Feb 2011; accepted 6 Mar 2011; published 18 Mar 2011

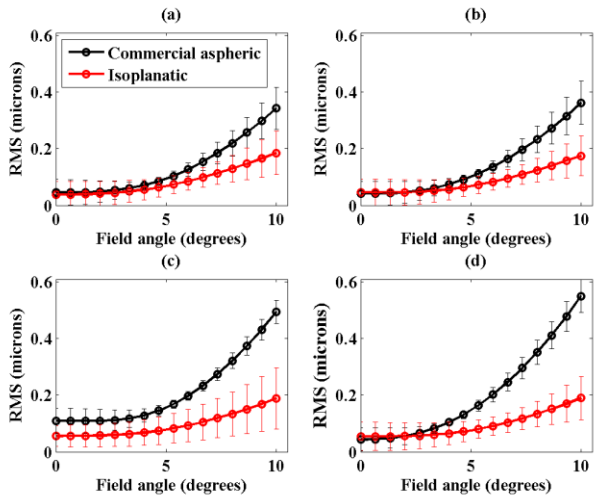

Fig. 7. RMS as a function of objective field angle for the new aspheric isoplanatic (red line) and commercial (black line), IOL designs of the Pharmacia b) Alcon c) B&L and d) Zeiss IOL platforms. Results are average across 6 eyes. Error bars stand for standard deviations.

Figure 8 compares the optical performance using the RMS and the Strehl ratio for the new aspheric isoplanatic designs for the different platforms. Whereas the Strehl ratio reveals more clearly the differences at low field angles, the RMS shows better the optical performance decay at large field angles.

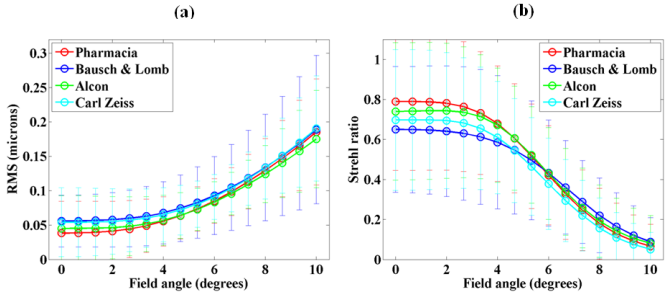

Fig. 8. (a) RMS and (b) Strehl ratio as a function of objective field angle for the new aspheric isoplanatic IOL designs of the Pharmacia (red line), Alcon (green line), B&L (blue line) and Zeiss (cyan line) IOL platforms. Error bars stand for standard deviations.

Figure 9 shows the optical performance of the aspheric SN60WF (Alcon) 19.5 D IOL compared to the new aspheric isoplanatic IOL for two fully anatomical pseudoaphakic eye models. As there is no rotational symmetry, these plots show optical quality as a function of the field angle, both in the horizontal (temporal-nasal) meridian (a)-(c) and in the vertical (inferior-superior) meridian (b)-(d). For eye #1 the fovea is located in the temporal-inferior direction (1.82, 4.06 deg), and for eye #2 towards the nasal-inferior direction (1.51, –5.92 deg). For both eyes the isoplanatic IOLs provide higher uniformity and better overall optical performance in both meridians across the visual field (average improvement of 18.1% in a 10 deg field).

#139474 - $15.00 USD Received 9 Dec 2010; revised 9 Feb 2011; accepted 6 Mar 2011; published 18 Mar 2011

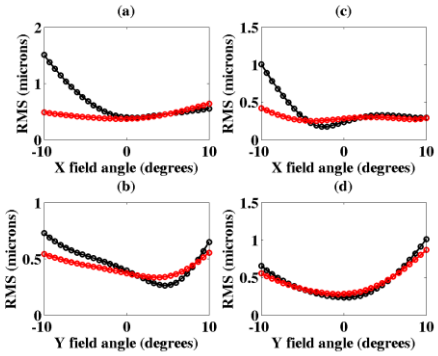

Fig. 9. RMS as a function of the object field angle of the SN60WF19.5 D IOL (black line) compared with the new isoplanatic Alcon IOL (red line) for two fully anatomical pseudoaphakic eye models: (a)-(b) model #1, OD (c)-(d) model #2, OS; (a) and (c) Horizontal meridian. (b) and (d) Vertical Meridian. Positive horizontal coordinates stand for nasal in right eyes, and temporal in left eyes, and viceversa

for negative horizontal coordinates. Positive vertical coordinates stand for superior and negative for inferior.

5. Discussion

5.1. The IOL design methodology

We have proposed an IOL design methodology which improves several aspects over current IOL design procedures. Each IOL manufacturer bases their IOL designs on different standardpseudoaphakic eye models. Pharmacia's one is based on the Gullstrand eye model with a modified cornea considering average keratometric data from a set of 16 corneas. Alcon used the so called Alcon-Navarro eye model [36]. Carl Zeiss used the Liou and Brennan eye model [3,42]. The B&L aspheric IOL design [37] does not require an eye model, as it is aimed at zero spherical aberration for a bundle of rays coming from infinity [37]. The diversity of eye models may partially contribute to the diversity of aspheric IOL monofocal designs.

We defined an anatomically plausible pseudophakic eye model. We used recent biometric data available in the literature, and an adaptive axial length and retina shape to different IOL powers. As shown in Fig. 3, a generic IOL designed with a general pseudoaphakic eye model generates different optical performances for different eyes. Ideally, customized eye models, with complete anatomical parameters, are the most appropriate to be used to design customized IOLs [1]. However, even in this case, knowledge is lacking from the post-operatively lens location, which has been proved to be a critical parameter in the refractive outcomes [1,43]. In any case, generic pseudoaphakic eye models for a specific IOL power are still justified because the standard deviations of the RMSs for the associate average values are relatively small.

RMS is a commonly used as metric in ophthalmic lens design although is not the optical quality metric that correlates best to final visual performance [39]. We observed that when using a retinal image quality based metric (Strehl ratio) the computation time increased dramatically and the convergence of the optimization procedure was not ensured. Nevertheless, comparisons of the optical performance in the evaluation of these lenses on six eyes were conducted both using the RMS and the Strehl ratio, showing (Fig. 8) a very close correspondence between both metrics. Further refinements applying a polychromatic geometrical metric could be applied with little extra complexity.

Pomerantzeff [44] found that the best optical performance across a 10° field, optimizing for a single angle of incidence, was achieved using an angle of 7.5 deg. However, we observed that using a single angle of incidence, though allowing fast computations, was not sufficient to achieve optimal and uniform performance across the field. A better approach, proposed by Bedggood et al [45], is to correct the aberrations for five different field positions,

#139474 - $15.00 USD Received 9 Dec 2010; revised 9 Feb 2011; accepted 6 Mar 2011; published 18 Mar 2011

one at 0° and the other four at 10° forming a cross pattern. Because we used a rotationally symmetric eye model, we selected five different angles along the same direction (0°, 2.5°, 5°, 7.5° & 10°). Interestingly, we found that the best distribution of relative weights for the different angle of incidences must give more weight to the central (0 °) and the extreme off-axis position (10 °). We can conclude that controlling aberrations in the extreme positions of the field of view of interest is the best strategy for isoplanatic IOL design, at least in the evaluated range.

5.2. State-of the art commercial IOLs

The optical performance of the aspheric commercial designs was significantly better, both on-axis and off-axis, than the corresponding spherical designs. These results are in agreement with previous experimental results [40,46]. It has been pointed out [40] that, although optical quality is significantly better with aspheric IOLs, tolerance to defocus tended to be lower with respect to spherical IOLs. We tested the tolerance to defocus error due to an incorrect estimation of the IOL position (± 0.5 mm from the expected IOL position) with the new isoplanatic designs. We found (average across the four platforms and field angles) that the absolute RMS difference was 0.094 μm and 0.168 μm for the new isoplanatic aspheric and spherical profiles respectively. Interestingly, the absolute impact of an axial IOL displacement is lower with aspheric designs, although the relative tolerance to the shift is higher with spherical designs.

We have shown that existing aspheric designs are more uniform across the field of view and pupil size than spherical designs, in most cases. Overall, Alcon and Pharmacia models provide significantly better performance than the Zeiss and Bausch and Lomb ones, indicating that the specific IOL surface profile is very relevant. The IOL platform and the constraints imposed by the material (refractive index) and physical dimensions (central and edge thickness) of the lens, may also play some role in the final optical outcomes.

5.3. The new isoplanatic IOLs

For the four platforms, we have found significantly better performances for the new aspheric IOL designs than for the state-of the art commercial designs, demonstrating the potentials of our new methodology for designing isoplanatic IOLs. The implementation of the new isoplanatic IOL designs could be easily achieved, as the designs are based on existing IOL platforms.

The benefits of using non spherical surfaces in IOL design have been widely reported. However, this is the first report, to our knowledge, that evaluates quantitatively the benefits of the aspheric over the conic surface design. On average, across the four platforms, using aspheric profiles allows 11.79% improvement of the optical quality with respect of using conic surfaces. This occurs because the use of high order aspheric coefficients provides additional degrees of freedom to reduce aberrations. In most cases, there is also an important improvement in *PSS* and in *FOV*. Interestingly, the best optical performance of commercial IOLs (Alcon and Pharmacia) is obtained with aspheric (and not conic) surfaces. In addition to the optical advantages of the aspheric surfaces, it has been suggested [47] that the use of aspheric surfaces could reduce the fabrication costs because less material has to be removed in the fabrication process. Conversely, the manufacture and interferometric testing of aspheric surfaces is more difficult than that of conic surfaces [47].

Several works [12] have suggested that posterior-convex IOLs are convenient to reduce off-axis aberrations. Moreover, an earlier study [44] suggested that: “the stronger curvature must face the cornea when the lens is calculated for the axial point, but it must face the retina when the lens is calculated for the best performance throughout the field of 10°”. In addition, curved posterior IOL surfaces are also convenient to reduce reflections and glare [20], and to reduce anisekonia effects in monocular IOL implantation [20]. Also, posterior-convex IOLs have been proposed to avoid cell migration, which induces posterior capsule opacification, by reducing the space between the posterior capsule and the posterior surface of the IOL [48].

#139474 - $15.00 USD Received 9 Dec 2010; revised 9 Feb 2011; accepted 6 Mar 2011; published 18 Mar 2011

Interestingly, the posterior surface of the human crystalline lens is also more curved than the anterior surface [49].

The above aspects suggest that IOLs designs with convexity facing the retina are more convenient. These type of designs, as the new isoplanatic IOL design based on the Acrysof platform (see Fig. 3), can be obtained allowing a large boundary constraint for the IOL vault. Also, for the aspheric surfaces, the boundary condition set to the vault strongly limits the complexity of the surface profiles. We observed that setting a high threshold for the vault we could optimize the optical results further. However, we applied a conservative vault threshold to avoid extremely complex profiles which could be limited by mechanical and manufacturing limitations.

Besides its visual impact, reducing off-axis optical aberrations has some other potential advantages, particularly the improvement of peripheral fundus imaging and of laser focusing in retinal photocoagulation therapy [50], in patients that may need fundus exploration or retinal treatments [51]. As shown in Fig. 9, when considering the interrelation between the IOL design and the biometric data, the optical outcomes depend on the specific pseudophakic eye model. This result again suggests that individual optical performance with IOLs will benefit from customized IOL design. Also, the level of defocus, caused by axial shifts of the actual IOL position with respect to the assumed position, is very relevant and can limit the improvements with the isoplanatic design. In highly realistic eye models, we found that the optical performance of the new isoplanatic design was clearly more uniform across the 10° field of view that for the state-of-the-art IOL and in addition the overall optical quality was also better. However, the interactions of asymmetrical aberrations, originated by corneal irregularities, tilt and decentrations, with the rotationally symmetric IOLs vary across individuals.

6. Conclusions

We have presented a new methodology for isoplanatic IOL design, i.e, uniform and optimized optical quality in a wide field of view (typically in a range of ten degrees).

The methodology introduces novelties in the definition of the pseudoaphakic eye model and the merit function. For each IOL design, the axial length and retina shape is changed according to the IOL power. The optimal merit function is the weighted sum of optical metrics (RMS of the wavefront) at five eccentricities across a 10 deg field, with maximum weights at 0 and 10 deg.

Aspheric IOLs provide significant optical improvement over IOLs based on conic (or spherical) surfaces. The new methodology allows the design of isoplanatic lenses, based on current commercial IOL platforms. The new aspheric isoplanatic IOLs improve the average optical quality and its uniformity across the field and pupil diameter over commercial aspheric designs.

Acknowledgments

We thank Juan Luis Rojas, Eva Larra and Pedro Salazar, from AJL Ophthalmics S.A., for motivating discussions. We acknowledge funding from “Ramon y Cajal” program (MICINN) to SB, FIS2008-02065 and PET-2006-0478 (MICINN, Spain), EURYI-05-102-ES (EUROHORCs-ESF) to SM; CSIC JAE-Intro to JM.

#139474 - $15.00 USD Received 9 Dec 2010; revised 9 Feb 2011; accepted 6 Mar 2011; published 18 Mar 2011